DOI: 10.1002/ejic.200700833

Metal–Organic Frameworks Containing Flexible Bis(benzimidazole) Ligands

Hui Jiang,[a] Jian-Fang Ma,*[a] Wen-Li Zhang,[a] Ying-Ying Liu,[a] Jin Yang,[a]
Guang-Ju Ping,[a] and Zhong-Min Su[a]

Keywords: Coordination polymers / Flexible ligands / Supramolecular chemistry / Luminescence

Eleven coordination polymers constructed from three structurally related flexible bis(benzimidazole) ligands, 1,1′-(1,4-butanediyl)bis(2-methylbenzimidazole) (L^1), 1,1′-(1,4-butanediyl)bis(2-ethylbenzimidazole) (L^2), and 1,1′-(1,4-butanediyl)bis(2-benzylbenzimidazole) (L^3), have been synthesized: $[Zn(cin)_2(L^1)]\cdot H_2O$ (**1**), $[Zn(cin)_2(L^2)]$ (**2**), $[Cd(cin)_2(L^1)]\cdot H_2O$ (**3**), $[Cd(cin)_2(L^2)]$ (**4**), $[Ag(MES)(L^1)_{0.5}]$ (**5**), $[Ag(MES)(L^2)_{0.5}]\cdot H_2O$ (**6**), $[Zn(adi)(L^1)]\cdot H_2O$ (**7**), $[Zn(adi)(L^2)_{0.5}]$ (**8**), $[Cd(adi)(L^1)]\cdot 2H_2O$ (**9**), $[Cd(adi)(L^2)]$ (**10**), and $[Cd(adi)(L^3)]\cdot 2H_2O$ (**11**), where cin = cinnamate anion, MES = 2-(*N*-morpholino)ethanesulfonate anion, and adi = adipate dianion. For compounds **1**–**4**, the cin anions are coordinated to metal ions in monodentate mode or bidentate chelating mode, and metal cations are bridged by L^1 or L^2 ligands to form 1-D chain structures. Compound **5** shows a 1-D chain structure which comprises a dimeric unit that is built from two silver ions and two MES anions. In compound **6**, silver ions are bridged by MES anions and L^2 ligands to form a 2-D (6, 3) network while compounds **7**–**9** possess 2D (4, 4) networks. In the structure of compound **8**, there exists a dimeric unit which is built from two zinc ions bridged by four carboxylate groups. Compound **10** exhibits a fourfold interpenetrating diamondoid net, and compound **11** displays a noninterpenetrating diamondoid framework. The luminescent properties for **1**–**11** are also discussed in detail.

Introduction

In the field of supramolecular chemistry, great interest has been focused on the crystal engineering of coordination frameworks due to their new topologies, intriguing architectures, intertwining phenomena, and potential applications.[1] Studies in this field have been focused on the design and construction of novel coordination frameworks and the relationships between their structures and properties. It is still a great challenge to predict the exact structures and compositions of the assembly products built by coordination bonds and/or hydrogen bonds in crystal engineering.[2] The construction of molecular architecture depends on the combination of several factors, such as the coordination nature of the metal ions, ligand structures, counterions, and so on. Therefore, systematic research on this topic is important for understanding the role of these factors in the formation of metal coordination frameworks.

The rigid ligands, such as 4,4′-bipyridine[3] and pyrazine,[4] have been extensively employed in the construction of a rich variety of intriguing architectures. However, there are an increasing number of recently characterized interesting interwoven frames incorporating with flexible ligands.[5] Ongoing research in our laboratory has been directed toward the design and synthesis of novel frameworks with flexible ligands.[6] To further investigate the influence of bis(benzimidazole) ligands on the formation of supramolecular architectures, in this paper, we have synthesized three flexible ligands: 1,1′-(1,4-butanediyl)bis(2-methylbenzimidazole) (L^1), 1,1′-(1,4-butanediyl)bis(2-ethylbenzimidazole) (L^2), and 1,1′-(1,4-butanediyl)bis(2-benzylbenzimidazole) (L^3) (Scheme 1). Three kinds of acids, cinnamic acid (Hcim), 2-(*N*-morpholino)ethanesulfonic acid (HMES), and adipic acid (H_2adi) (Scheme 2) are selected as anions for the reason that their coordination chemistry has rarely been investigated.[7]

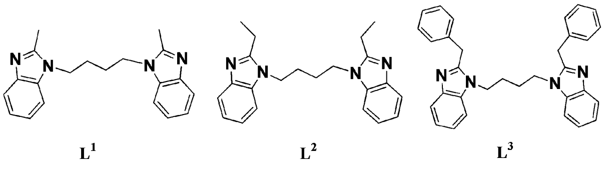

Scheme 1.

In this work, 11 coordination polymers, namely, $[Zn(cin)_2(L^1)]\cdot H_2O$ (**1**), $[Zn(cin)_2(L^2)]$ (**2**), $[Cd(cin)_2(L^1)]\cdot H_2O$ (**3**), $[Cd(cin)_2(L^2)]$ (**4**), $[Ag(MES)(L^1)_{0.5}]$ (**5**), $[Ag(MES)(L^2)_{0.5}]\cdot H_2O$ (**6**), $[Zn(adi)(L^1)]\cdot H_2O$ (**7**), $[Zn(adi)(L^2)_{0.5}]$ (**8**), $[Cd(adi)(L^1)]\cdot 2H_2O$ (**9**), $[Cd(adi)(L^2)]$ (**10**), and $[Cd(adi)(L^3)]\cdot 2H_2O$ (**11**), have been synthesized by both solution and solvothermal reactions. The crystal structures of these

---

[a] Key Lab of Polyoxometalate Science, Department of Chemistry, Northeast Normal University,
Changchun 130024, People's Republic of China
Fax: +86-431-85098620
E-mail: jianfangma@yahoo.com.cn

Supporting information for this article is available on the WWW under http://www.eurjic.org or from the author.

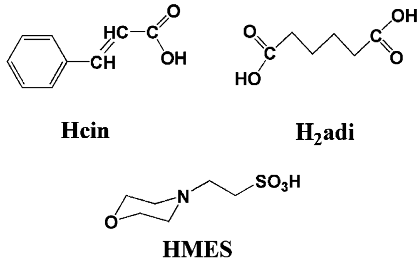

Scheme 2.

compounds and topological analyses, along with the systematic investigation of the modulated effect of bis(benzimidazole) ligands on the ultimate frameworks, will be represented and discussed in this paper.

Results and Discussion

Syntheses of the Compounds

As is well known, the reactions of metal ions with carboxylates or sulfonates and neutral ligands in aqueous solution often result in the formation of insoluble substances, presumably because of the fast coordination of them to form polymeric structures. In this paper, solution reaction and solvothermal synthesis were used to synthesize the compounds. Compounds **5** and **6** are insoluble in water and common organic solvents, but they can be dissolved in a concentrated solution of ammonia by segregating the ligands from metal cations. The crystals of these compounds were obtained by using a crystallization process through evaporating an ammoniacal solution of them. Compounds **1**–**4** and **7**–**11** were synthesized by solvothermal synthesis. All compounds are stable in air and are insoluble in common solvents such as ethanol, benzene, acetone, and acetonitrile.

Descriptions of Crystal Structures

Structure Description of 1

In the structure of **1**, each zinc ion is coordinated by two nitrogen atoms from two L^1 ligands and two oxygen atoms from two cin anions, showing a distorted tetrahedral coordination geometry (Figure 1, a). The Zn(1)–N distances of 2.033(2) Å and the Zn(1)–O distances of 1.951(2) Å fall in the range of normal Zn–N and Zn–O distances.[8,9] Each cin anion coordinates to one zinc center through one carboxylate O atom, and the zinc ions are bridged by L^1 ligands to form an infinite chain (Figure 1, b). There exist lattice water molecules in the structure of **1**. The water molecule donates hydrogen bonds to the carboxylate O atoms of the cin anion. The geometric parameters of the hydrogen bonds are summarized in Table 1. As is well known, a water molecule has two hydrogen atoms and two lone-electron pairs which enable it to participate in four hydrogen bonds in a tetrahedral configuration, but it often shows a three-coordinate configuration.[10a,10b] For compound **1**, the water molecule shows a two-coordinate mode.[10c,11a]

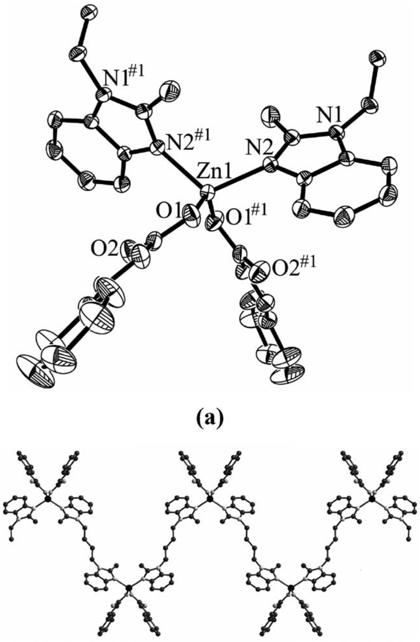

Figure 1. (a) ORTEP diagram showing the coordination environment for the Zn atom in **1**. (b) The infinite 1-D zigzag chain of **1**.

Table 1. Selected hydrogen-bonding geometry data [Å, deg].

D–H···A	d(D–H)	d(H···A)	d(D···A)	∠(D–H···A)
	Compound **1**			
O(1W)–H(1A)···O(2)	0.93(5)	2.16(15)	2.876(6)	133(16)
	Compound **3**			
O(W1)–H(1A)···O(1)	0.99(7)	1.97(7)	2.960(8)	173(11)
	Compound **6**			
O(1W)–H(1A)···O(4)$^{\#3}$	0.90(5)	2.01(5)	2.866(4)	158(4)
O(1W)–H(1B)···O(3)	0.93(5)	1.82(5)	2.717(4)	162(4)
	Compound **9**			
O(1W)–H(1B)···O(3)	0.83(5)	2.05(6)	2.796(5)	150(9)
O(1W)–H(1A)···O(2W)	0.91(5)	1.94(5)	2.797(6)	156(8)
O(2W)–H(2A)···O(2)$^{\#5}$	0.91(5)	1.97(5)	2.777(5)	147(6)
O(2W)–H(2B)···O(1 W)$^{\#6}$	0.88(4)	2.31(5)	3.110(8)	151(6)

Symmetry codes for **6**: $^{\#3}$ $-x + 5/2$, $y + 1/2$, $-z - 1/2$; **9**: $^{\#5}$ $-x + 2$, $-y + 1$, $-z$; $^{\#6}$ $-x + 2$, $-y + 2$, $-z$.

Structure Description of 2

The structure of **2** is similar to that of compound **1** except L^1 is replaced by L^2. Part of the structure of **2** is shown in Figure 2. The Zn–O and Zn–N bond lengths and related angles for **1** and **2** are slightly different. Zinc ions are bridged by L^2 ligands to form a 1D chain the same as that observed in compound **1** (see Figure S1, Supporting Information).

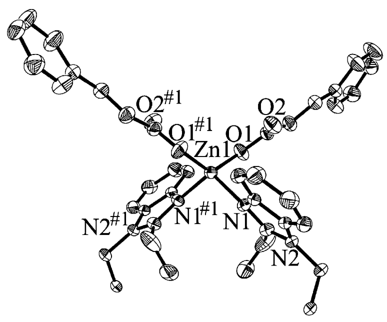

Figure 2. ORTEP diagram showing the coordination environment for the Zn atom in **2**.

Structure Description of 3

In the structure of **3**, each cadmium center is coordinated by two nitrogen atoms [Cd–N 2.261(3) Å] from two L^1 ligands and four carboxylate O atoms [Cd–O 2.339(6)–2.526(6) Å] from two cin anions (Figure 3, a). The geometry around the cadmium center can be described as a distorted octahedron. The Cd–O distances are quite similar to the normal Cd–O distances.[12] The cin anion in **3** exhibits a bidentate chelating coordination mode. Cadmium centers are bridged by L^1 ligands to form a 1-D infinite zigzag chain (Figure 3, b).

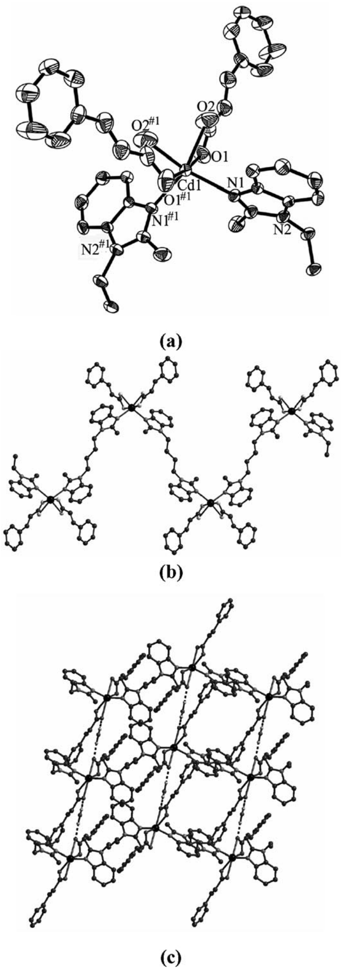

Figure 3. (a) ORTEP diagram showing the coordination environment for the Cd atom in **3**. (b) The infinite 1-D zigzag chain of **3**. (c) The 2-D layer containing hydrogen bonds between cin anions and water molecules of **3** (H-bonds: dashed lines).

In the structure of **3**, there exist lattice water molecules which show a two-coordinate mode (Table 1). The adjacent polymeric chains are bridged by the hydrogen-bonding interactions between the water molecules and the carboxylate oxygen atoms to form a wavelike 2-D supramolecular layer (Figure 3, c). These layers stack in a parallel mode to form the overall structure of **3** (Figure S2).

Structure Description of 4

In the structure of **4**, each cadmium center is coordinated by four oxygen atoms from two cin anions and two nitrogen atoms from two L^2 ligands, showing a distorted octahedral geometry (Figure 4, a). The cin anion adopts a bidentate chelating coordination mode, and Cd^{II} atoms are connected by L^2 ligands to form a 1-D zigzag chain (Figure 4, b). The polymeric chains are arranged in a parallel mode to form a 2D sheet (Figure S3).

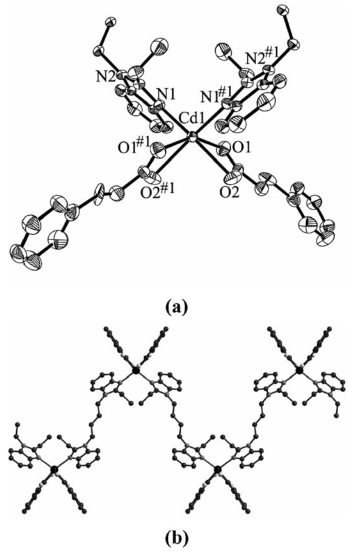

Figure 4. (a) ORTEP diagram showing the coordination environment for the Cd atom in **4**. (b) The infinite 1-D zigzag chain of **4**.

Structure Description of 5

As shown in part a of Figure 5, the silver ion in **5** is coordinated by two oxygen atoms [Ag–O 2.479(2)–2.516(2) Å] from two MES anions and two nitrogen atoms [Ag–N 2.155(2)–2.285(2) Å] from one MES anion and one L^1 ligand, showing a distorted tetrahedral coordination geometry. The Ag–O bond lengths are similar to the values in the related compound.[13]

As illustrated in part b of Figure 5, the coordination of MES anion to silver ion results in a $[Ag_2(MES)_2]$ unit with two kinds of rings. The eight-membered ring ($Ag_2O_4S_2$) is composed of two silver ions and two sulfonate groups, with the Ag···Ag distance of 7.06 Å, while the six-membered ring is formed by one silver ion and one MES anion. The $[Ag_2(MES)_2]$ units are linked by L^1 ligands to form a 1-D chain structure (Figure 5, c). Compound **5** displays a unique supramolecular organization of the polymeric chains. These polymeric chains are arranged on parallel levels in different propagating directions, rotated by 72.5° on passing from one level to the successive one, thus resulting in an ABAB sequence (Figure 5, d). Similar packing fashions of 1-D chain polymers have rarely been observed.[11]

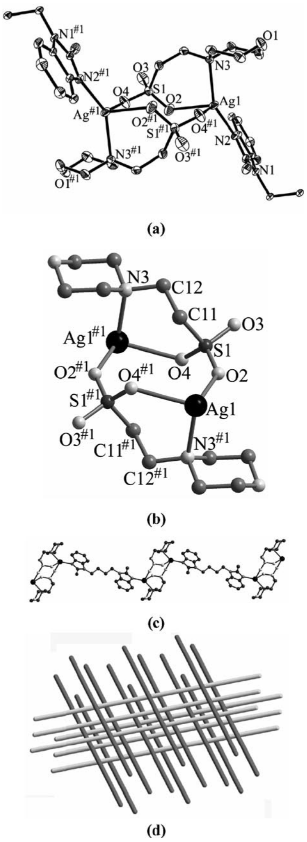

Figure 5. (a) ORTEP diagram showing the coordination environment for the Ag atom in **5**. (b) View of the dimeric unit consisting of two Ag ions and two MES anions. (c) The infinite 1D chain of **5**. (d) Rod-packing diagram of the 1D chains spanning two different directions (light gray and medium gray) in **5**.

Structure Description of 6

In the structure of **6**, the silver ion is coordinated by one oxygen atom from one MES anion and two nitrogen atoms from one MES anion and one L^2 ligand, showing a distorted T-shaped geometry (Figure 6, a). The silver ions are bridged by MES anions to form a 1-D polymeric chain (Figure 6, b). These chains are further extended by L^2 ligands to result in a 2-D (6, 3) network (Figure 6, c). The 2-D polymeric networks stack in a parallel mode to form the overall structure of **6** (Figure S4). The lattice water molecules are hydrogen-bonded to the oxygen atoms of the MES anions.

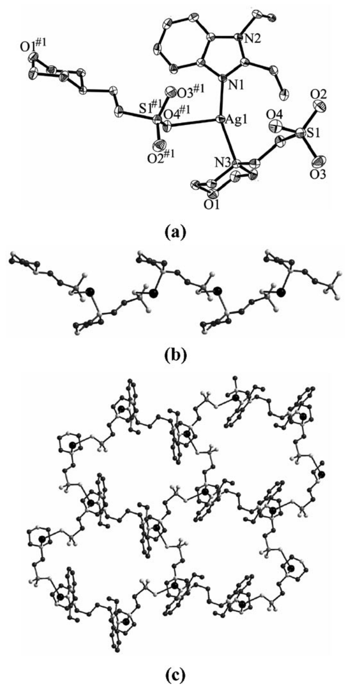

Figure 6. (a) ORTEP diagram showing the coordination environment for the Ag atom in **6**. (b) The infinite 1-D zigzag chain composed of silver ions and MES anions. (c) View of the 2-D (6, 3) network.

Structure Description of 7

In compound **7**, the zinc ion is coordinated by two oxygen atoms [Zn–O 1.955(5)–1.979(5) Å] from two monodentate adi anions and two nitrogen atoms [Zn–N 2.048(5)–2.050(5) Å] from two L^1 ligands (Figure 7, a), showing a distorted tetrahedral geometry. The zinc ions are bridged by adi anions to form an infinite chain, and these chains are connected by L^1 ligands to form a 2-D wavelike (4, 4) network (Figure 7, b).

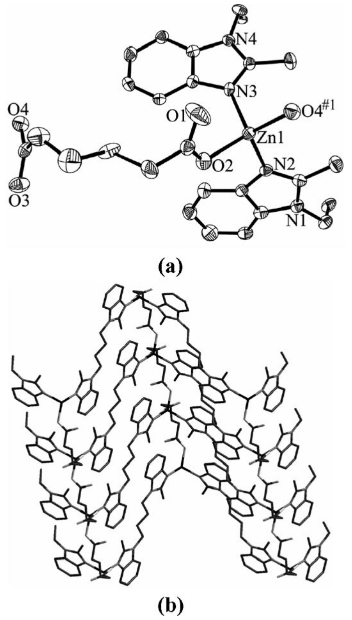

Figure 7. (a) ORTEP diagram showing the coordination environment for the Zn atom in **7**. (b) The 2-D wavelike polymeric layer.

Structure Description of 8

In the structure of **8**, the zinc center is coordinated by four oxygen atoms from four adi anions and one nitrogen atom from a L^2 ligand to furnish a distorted square-pyramidal geometry (Figure 8, a). Each adi anion is coordinated to four zinc ions, adopting a bis(bidentate-bridging) coordination mode. A pair of Zn^{II} ions are bridged by four carboxylate groups from four adi anions to give a dinuclear $[Zn_2(CO_2)_4]$ unit in which the Zn···Zn distance is 3.01 Å. The $[Zn_2(CO_2)_4]$ units are linked by adi anions to form a double-chain structure (Figure 8, b). These chains are further connected by L^2 ligands to form a 2-D (4, 4) network (Figure 8, c).

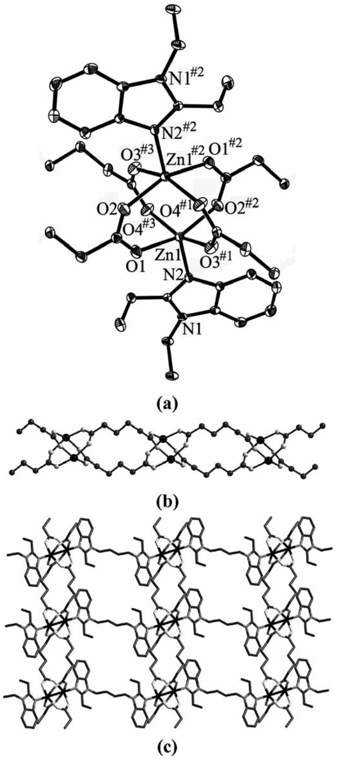

Figure 8. (a) ORTEP diagram showing the coordination environment for the Zn atom in **8**. (b) The infinite 1-D double chain composed of Zn ions and adi anions. (c) View of the 2D layer.

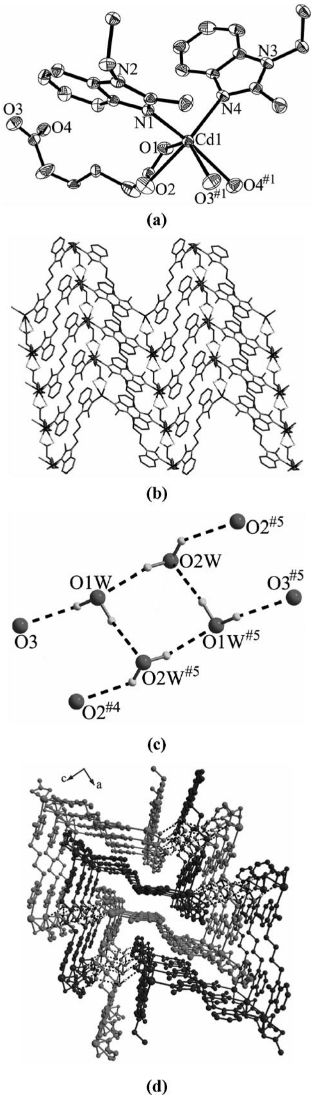

Figure 9. (a) ORTEP diagram showing the coordination environment for the Cd atom in **9**. (b) The infinite 2-D wavelike layer. (c) View of the $(H_2O)_4$ cluster. (d) The packing diagram of **9** (dashed lines represent hydrogen bonds).

Structure Description of 9

In compound **9**, the cadmium ion is six-coordinate by two nitrogen atoms from two L^1 ligands and four carboxylate O atoms from two adi anions, showing a distorted octahedral geometry (Figure 9, a). Cadmium ions are bridged by the bis(bidentate-chelating) adi anions to form an infinite chain. These chains are further connected by L^1 ligands to form a 2-D wavelike (4, 4) network (Figure 9, b).

In the structure of **9**, there exist $(H_2O)_4$ clusters (Figure 9, c). Hydrogen bond data indicate that O1W donates hydrogen bonds to the carboxylate oxygen atom (O3) and water molecule ($O2W^{\#5}$) which in turn donates to $O2^{\#4}$ and $O1W^{\#5}$. The polymeric layers are linked by hydrogen-bonding interactions to form two interpenetrating 3-D supramolecular structures (Figure 9, d).

Structure Description of 10

In the structure of **10**, the cadmium center is coordinated by two nitrogen atoms from two L^2 ligands and four oxygen atoms from two adi anions, showing a distorted octahedral geometry (Figure 10, a). The topological analysis of **10** reveals that it is a typically diamondoid framework containing large adamantanoid cages (Figure 10, b).[11c] The Cd···Cd distances separated by the adi anion and L^2 ligand are 11.39 and 14.50 Å, respectively. In order to minimize the big void cavities and stabilize the framework, the potential voids formed by a single 3D network show incorporation of another three identical networks, thus giving a fourfold interpenetrating diamondoid array (Figure 10, c). This kind of fourfold interpenetrating structure has been described in previous reports.[14]

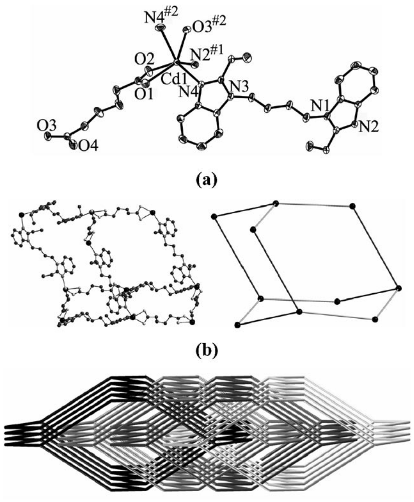

(a)

(b)

(c)

Figure 10. (a) ORTEP diagram showing the coordination environment for the Cd atom in **10**. (b) Single adamantanoid cage. (Light gray lines represent the adi ligands and dark gray lines represent the L^2 ligands). (c) View of the fourfold interpenetrating diamondoid framework.

Structure Description of 11

In compound **11**, the cadmium ion is coordinated by four oxygen atoms from two adi anions and two nitrogen atoms from two L^3 ligands, showing a distorted octahedral geometry (Figure 11, a). Each adi anion is coordinated to two Cd ions, adopting a bis(bidentate-chelating) coordination mode.[15] The topological analysis of **11** reveals that it is also a diamondoid framework (Figure 11, b). In principle, the exploration of long ligands usually leads to large voids that may further result in interpenetrating or entangled structures. It is somewhat unexpected that no interpenetration occurs between the networks of **11**. This may be caused by the existence of the bulky benzyl groups of the L^3 ligand. There exist π-π stacking interactions between the phenyl rings and benzimidazole rings of adjacent L^3 ligands, with the centroid-to-centroid distance of 3.65 Å and face-to-face distance of 3.40 Å (Figure 11, c).

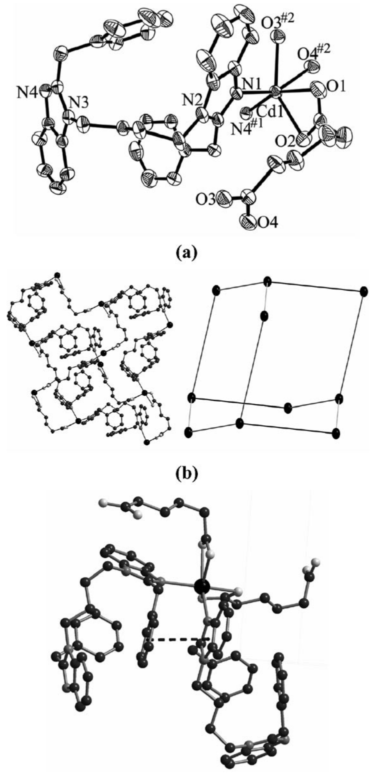

(a)

(b)

(c)

Figure 11. (a) ORTEP diagram showing the coordination environment for the Cd atom in **11**. (b) Single adamantanoid cage. (Light gray lines represent the adi ligands and dark gray lines represent the L^2 ligands). (c) View of the π-π interaction.

The Effect of the Neutral Ligands on the Structure of the Complexes

L^1–L^3 show similar structural features and display the same bidentate bridging coordination mode with two aromatic N atoms coordinating to two different metal ions in compounds **1**–**11**. The similar frameworks may be expected when L^1, L^2, and L^3 are used, respectively. Indeed, compounds **1** and **2** have similar structures; and compounds **3** and **4** also show similar frameworks.

However, sometimes changes in the substituting groups in the 2- and 2′-positions of the bis(benzimidazole) ligands can result in changes in several aspects of the final frameworks.

1. A change in dimensionalities for the coordination polymers. Compounds **9** and **10** contain the same cadmium ion and the same adi anion, and all adi anions display the same coordination mode with each carboxylate group chelating one cadmium ion. The replacement of the methyl group by the ethyl group results in the change of frameworks from the 2-D (4, 4) net to the 3-D diamondoid framework through the fusion of the adjacent layers of **9**. A change of dimensionalities also occurs in compounds **5** and **6**.
2. A change in interpenetrations for the frameworks. Although both compounds **10** and **11** display the same diamondoid framework, the replacement of the ethyl group by the benzyl group results in a change from the fourfold interpenetrating framework of **10** to the noninterpenetrating framework of **11** due to the larger volume of the benzyl group compared to the ethyl group.
3. A change in M/L ratios for the compounds. The similar synthetic conditions gave two compounds **7** and **8** with different M/L ratios (1:1 for **7** and 2:1 for **8**) due to the change of the substituting groups from the methyl to the ethyl group.
4. A change in coordination modes of the anions. For compounds **5** and **6**, the change of the substituting groups from the methyl to the ethyl group results in a change of the coordination modes for the MES anions. A similar change also occurred in **7** and **8**.

The Effect of the Anions on the Structure of the Complexes

From the structures of **1**–**11**, it can be seen that the anions play a very important role in the construction of the frameworks. The cin anion contains one carboxylate group, and coordinates to only one metal ion, acting as a terminal ligand. And the related complexes (**1**–**4**) contain only one kind of connector (L^1 or L^2), and show 1-D chain structures. The adi anion contains two carboxylate groups, acting as a bridging ligand. Complexes **7**–**11** have two kinds of bridging ligands [adi anion and bis(benzimidazole) ligand], and display 2-D or 3-D polymeric structures. The MES anion adopts two kinds of coordination modes. Compound **6** exhibits a 2-D polymeric structure, with the MES anion acting as a bidentate bridging ligand. In compound **5**, the MES anion acts as an interesting tridentate ligand, and silver ions are linked by MES anions to form dinuclear subunits that are further bridged by bidentate L^1 ligands to form a 1-D chain structure.

The Effect of the Metal Ions on the Structure of the Complexes

From the structures of compounds **1**–**11**, it can be seen that the coordination behavior of metal ions have a great influence on the structures of the complexes. In compounds **1**–**11**, the metal ions display a variety of coordination numbers (from 3 to 6). Both Zn^{II} and Cd^{II} ions have a closed d^{10} electronic shell, and there is no crystal field stabilization energy for them when their complexes are formed. The coordination numbers of Zn^{II} and Cd^{II} ions are mainly determined by the steric repulsion between different ligands. Since the radius of the Cd^{II} ion is larger than that of the Zn^{II} ion, the coordination numbers of the Cd^{II} ions in **3**, **4**, and **9**–**11** are larger than those of the Zn^{II} ions in **1**, **2**, **7**, and **8**. Although the radius of the Ag^{I} ion is larger than that of the Cd^{II} ion, the coordination numbers of the Ag^{I} ions in **5** and **6** are lower than those of the Cd^{II} ions because the Ag^{I} ion and Cd^{II} ion have different valences.

On the basis of the above discussion, many factors, such as the stoichiometric ratio of the components, the radii of metal ions, the versatility of the metal coordination geometries, and the donor characters of nitrogen and oxygen atoms to the metals, play fundamental roles in the formation of the final products. Since these factors work together to affect the structures, it is difficult to separate and rationalize them, and it is hard to propose definitive reasons as to why each compound adopts a different configuration with our present state of knowledge.

Thermal Analysis

In order to characterize the compounds more fully in terms of thermal stability, their thermal behaviors were studied by thermogravimetric analysis (TGA). The experiments were performed on samples consisting of numerous single crystals of **1**, **3**, **7**, **9**, and **11** under N_2 atmosphere with a heating rate of 10 °C/min (Figures S5–S9 and Table S2 in the Supporting Information).

For compound **1**, the weight loss corresponding to the release of water molecules is observed from room temperature to 97 °C (obsd. 2.0%, calcd. 2.6%). The anhydrous compound begins to decompose at 240 °C. For compound **3**, the weight loss corresponding to the release of water molecules is observed from room temperature to 149 °C (obsd. 2.4%, calcd. 2.7%). The anhydrous compound begins to decompose at 278 °C. The TGA curve of **7** shows that it undergoes dehydration in the range of 52–83 °C (obsd. 2.7%, calcd. 3.3%). The decomposition of the anhydrous compound occurs at 231 °C. For compound **9**, the weight loss in the range of room temperature to 100 °C corresponds to the departure of water molecules (a weight loss of 2.1% is smaller than the calculated value, 5.9%, probably resulting from a very slow liberation of the water molecules from **9** at room temperature).[16] For compound **11**, the weight loss in the range of 60–255 °C corresponds to the departure of water molecules (obsd. 3.0%, calcd. 4.7%). The removal of the organic components occurs at 283 °C.

Luminescent Properties

Luminescent compounds are of great current interest because of their various applications in chemical sensors, photochemistry, and electroluminescent (EL) display.[17] The photoluminescent properties of compounds **1**–**11** were studied at room temperature. The solid-state photoluminescent spectra of **1**–**11**, and L^1–L^3 are depicted in Figure S10. The wavelengths of the emission maxima and excitation are listed in Table 2.

Table 2. Wavelengths λ [nm] of the emission maxima and excitation.

Compound	**1**	**2**	**3**	**4**	**5**	**6**
λ_{em}	423	465	438	408	479	363
λ_{ex}	358	405	375	358	420	296
Compound	**7**	**8**	**9**	**10**	**11**	
λ_{em}	412, 441	390	365, 441	360	445	
λ_{ex}	280	332	292	295	396	

The free L^1, L^2, and L^3 ligands display luminescence with emission maxima at 371, 365, and 413 nm (λ_{ex} = 295 nm for L^1 and L^2, λ_{ex} = 340 nm for L^3), respectively, which are attributed to the $\pi\rightarrow\pi^*$ transitions. The free Hcin shows an emission maximum at 365 nm with two shoulder peaks at 384 and 405 nm (Figure S11). The emission peaks of compounds **1**–**5**, **7**–**9**, and **11** are attributed to charge transfer transition and the intraligand transition.[18,19] For compounds **1**–**5**, **8**, and **11**, the emission peaks of charge transfer transition and the intraligand transition are mixed together, showing only one emission peak. Compounds **7** and **9** exhibit a main peak with a shoulder at 412 and 441 nm for **7**, and 365 and 441 nm for **9** upon excitation at 280 and 292 nm, respectively. The peaks at 412 and 365 nm would be assigned to intraligand transitions of bis(benzimidazole) ligands, while the shoulder peaks at 441 nm may be attributed to the emission of charge transfer transitions. The emission peaks of compounds **6** and **10** are probably due to $\pi\rightarrow\pi^*$ transitions of L^2 ligands because similar peaks also appear for the free bis(benzimidazole) ligands.

Conclusions

In summary, 11 coordination polymers based on L^1–L^3 ligands and three different anions have been synthesized and characterized. The results of this study not only illustrate that the changes of the substituting groups of bis(benzimidazole) ligands play an important role in the construction of coordination polymers, but also illustrate that the coordination modes of anions and the coordination behavior of metal ions can also have an influence on the final frameworks. It is anticipated that more metal complexes containing flexible divergent ligands with interesting structures as well as physical properties will be synthesized.

Experimental Section

General: All reagents and solvents for syntheses were purchased from commercial sources and used without further purification. The C, H, and N elemental analysis was conducted with a Perkin–Elmer 240C elemental analyzer. The FT-IR spectra were recorded from KBr pellets in the range 4000–400 cm^{-1} on a Mattson Alpha-Centauri spectrometer. TGA was performed with a Perkin–Elmer TG-7 analyzer heated from room temperature to 600 °C under nitrogen. The solid-state luminescent properties of compounds **1**–**11** were measured with a Perkin–Elmer LS55 spectrometer at room temperature.

Synthesis of 1,1′-(1,4-Butanediyl)bis(2-methylbenzimidazole) (L^1): A mixture of NaOH (1.18 g, 30 mmol) and 2-methylbenzimidazole (3.96 g, 30 mmol) in acetone (50 mL) was stirred at room temperature to give a clear solution, then 1,4-dibromobutane (3.24 g, 15 mmol) and NaI (0.1 g) were added. The mixture was stirred at 50 °C for 10 h. After removing the acetone, 50 mL of water was added and a brown solid formed. The solid was recrystallized from a mixture of water and ethanol (4:1, v/v) to give L^1 as a light brown crystalline solid. Yield 85% based on 2-methylbenzimidazole.

Synthesis of 1,1′-(1,4-Butanediyl)bis(2-ethylbenzimidazole) (L^2): The same synthetic method as for L^1 was used except that 2-methylbenzimidazole was replaced by 2-ethylbenzimidazole (4.38 g, 30 mmol). Yield 80% based on 2-ethylbenzimidazole.

Synthesis of 1,1′-(1,4-Butanediyl)bis(2-benzylbenzimidazole) (L^3): The same synthetic method as for L^1 was used except that 2-methylbenzimidazole was replaced by 2-benzylbenzimidazole (6.25 g, 30 mmol). Yield 78% based on 2-benzylbenzimidazole.

Synthesis of [Zn(cin)$_2$(L^1)]·H$_2$O (1): A mixture of ZnCO$_3$ (0.025 g, 0.2 mmol), Hcin (0.059 g, 0.4 mmol), L^1 (0.064 g, 0.2 mmol) in EtOH/H$_2$O (1:4, v/v) (10 mL) was placed in a Teflon reactor. The mixture was heated at 180 °C for 3 d, and then it was gradually cooled to room temperature at a rate of 10 °C h^{-1}. Colorless crystals of **1** were obtained. Yield 50% based on ZnCO$_3$ (0.070 g). $C_{38}H_{38}N_4O_5Zn$ (696.09): calcd. C 65.57, H 5.50, N 8.05; found C 65.30, H 5.65, N 8.25. IR (KBr): $\tilde{\nu}$ = 3726 (w), 1645 (s), 1605 (m), 1497 (w), 1461 (m), 1417 (m), 1362 (s), 1012 (w), 978 (m), 749 (s), 685 (w) cm^{-1}.

Synthesis of [Zn(cin)$_2$(L^2)] (2): A mixture of ZnCO$_3$ (0.025 g, 0.2 mmol), Hcin (0.059 g, 0.4 mmol), L^2 (0.069 g, 0.2 mmol) in EtOH/H$_2$O (1:4, v/v) (10 mL) was placed in a Teflon reactor. The mixture was heated at 170 °C for 3 d, and then it was gradually cooled to room temperature at a rate of 10 °C h^{-1}. Colorless crystals of **2** were obtained. Yield 53% based on ZnCO$_3$ (0.075 g). $C_{40}H_{40}N_4O_4Zn$ (706.13): calcd. C 68.04, H 5.71, N 7.93; found C 68.02, H 5.75, N 8.01. IR (KBr): $\tilde{\nu}$ = 3416 (w), 2979 (w), 2939 (w), 1687 (m), 1642 (s), 1610 (m), 1577 (m), 1465 (s), 1357 (s), 1306 (s), 1280 (m), 1191 (s), 1012 (w), 982 (m), 749 (s), 711 (w), 682 (w) cm^{-1}.

Synthesis of [Cd(cin)$_2$(L^1)]·H$_2$O (3): A mixture of Cd(OH)$_2$ (0.035 g, 0.2 mmol), Hcin (0.059 g, 0.4 mmol), and L^1 (0.064 g, 0.2 mmol) in EtOH/H$_2$O (1:4, v/v) (10 mL) was placed in a Teflon reactor (15 mL). The mixture was heated at 160 °C for 3 d, then it was gradually cooled to room temperature at a rate of 10 °C h^{-1}. Colorless crystals of **3** were obtained. Yield 56% based on Cd(OH)$_2$ (0.083 g). $C_{38}H_{38}CdN_4O_5$ (743.12): calcd. C 61.42, H 5.15, N 7.54; found C 61.29, H 5.05, N 7.49. IR (KBr): $\tilde{\nu}$ = 3737 (m), 3680 (w), 3622 (w), 1742 (w), 1692 (m), 1645 (s), 1547 (s), 1513 (s), 1462 (m), 1397 (s), 1244 (w), 744 (w), 677 (s) cm^{-1}.

Synthesis of [Cd(Cin)$_2$(L^2)] (4): The same synthetic method as for **3** was used except that L^1 was replaced by L^2 (0.070 g, 0.2 mmol). Yield 50% based on Cd(OH)$_2$ (0.075 g). $C_{40}H_{40}CdN_4O_4$ (753.16): calcd. C 63.79, H 5.35, N 7.44; found C 63.68, H 5.26, N 7.49. IR (KBr): $\tilde{\nu}$ = 3847 (w), 3736 (m), 3680 (m), 3621 (m), 1742 (w), 1693 (m), 1644 (s), 1547 (s), 1512 (s), 1462 (s), 1391 (s), 1242 (m), 1066 (w), 745 (m), 678 (s) cm^{-1}.

Synthesis of [Ag(MES)(L^1)$_{0.5}$] (5): A mixture of Ag$_2$CO$_3$ (0.028 g, 0.1 mmol), HMES (0.043 g, 0.2 mmol), and L^1 (0.032 g, 0.1 mmol) in ethanol (10 mL) was stirred for 30 min at room temperature. The mixture was dissolved by dropwise addition of ammonia (5 M). Colorless single crystals were obtained by slow evaporation of the solution at room temperature. Yield 66% based on Ag$_2$CO$_3$ (0.030 g). $C_{16}H_{23}AgN_3O_4S$ (461.30): calcd. C 41.66, H 5.03, N 9.11; found C 41.68, H 5.04, N 9.09. IR (KBr): $\tilde{\nu}$ = 3848 (m), 3738 (s), 3680 (m), 3619 (m), 2925 (m), 2801 (m), 2470 (w), 1741 (w), 1686 (m), 1645 (s), 1548 (s), 1513 (s), 1464 (m), 1060 (s), 672 (s), 630 (w), 487 (w) cm^{-1}.

Synthesis of [Ag(MES)(L^2)$_{0.5}$]·H$_2$O (6): The same synthetic method as for **5** was used except that L^1 was replaced by L^2 (0.035 g, 0.1 mmol). Yield 68% based on Ag$_2$CO$_3$ (0.034 g). $C_{17}H_{27}AgN_3O_5S$ (493.35): calcd. C 41.39, H 5.52, N 8.52; found C 41.48, H 5.64, N 8.78. IR (KBr): $\tilde{\nu}$ = 3829 (m), 3736 (s), 3620 (m), 3034 (m), 2933 (s), 1611 (w), 1513 (s), 1462 (s), 1408 (s), 1367 (m), 1323 (w), 1245 (w), 1152 (w), 747 (w), 672 (w) cm^{-1}.

Synthesis of [Zn(adi)(L^1)]·H$_2$O (7): A mixture of ZnCO$_3$ (0.025 g, 0.2 mmol), H$_2$adi (0.029 g, 0.2 mmol), L^1 (0.064 g, 0.2 mmol) in EtOH/H$_2$O (1:4, v/v) (10 mL) was placed in a Teflon reactor. The mixture was heated at 180 °C for 3 d, and then it was gradually cooled to room temperature at a rate of 10 °C h^{-1}. Colorless crystals of **7** were obtained. Yield 50% based on ZnCO$_3$ (0.055 g). $C_{26}H_{32}N_4O_5Zn$ (545.93): calcd. C 57.20, H 5.91, N 10.26; found C 55.30, H 6.05, N 9.89. IR (KBr): $\tilde{\nu}$ = 3736 (w), 3621 (w), 3444 (m), 2941 (m), 2864 (w), 1614 (s), 1512 (s), 1463 (s), 1389 (s), 1288 (m), 1244 (m), 1014 (m), 938 (w), 851 (w), 745 (s), 672 (m), 430 (m) cm^{-1}.

Synthesis of [Zn(adi)(L^2)$_{0.5}$] (8): A mixture of ZnCO$_3$ (0.025 g, 0.2 mmol), H$_2$adi (0.029 g, 0.2 mmol), L^2 (0.069 g, 0.2 mmol) in EtOH/H$_2$O (1:4, v/v) (10 mL) was placed in a Teflon reactor. The mixture was heated at 160 °C for 3 d, and then it was gradually cooled to room temperature at a rate of 10 °C h^{-1}. Colorless crystals of **8** were obtained. Yield 54% based on ZnCO$_3$ (0.041 g). $C_{17}H_{21}N_2O_4Zn$ (382.73): calcd. C 53.35, H 5.53, N 7.32; found C 53.30, H 5.52, N 7.34. IR (KBr): $\tilde{\nu}$ = 3894 (w), 3847 (w), 3736 (s), 3621 (m), 1836 (w), 1742 (m), 1692 (s), 1647 (s), 1513 (s), 1532 (s), 1548 (s), 1463 (m), 1389 (m), 675 (s) cm^{-1}.

Synthesis of [Cd(adi)(L^1)]·2H$_2$O (9): A mixture of Cd(OH)$_2$ (0.035 g, 0.2 mmol), H$_2$adi (0.029 g, 0.2 mmol), L^1 (0.064 g, 0.2 mmol) in EtOH/H_2O (1:4, v/v) (10 mL) was placed in a Teflon reactor. The mixture was heated at 160 °C for 3 d, and then it was gradually cooled to room temperature at a rate of 10 °C h^{-1}. Colorless crystals of **9** were obtained. Yield 50% based on $Cd(OH)_2$ (0.070 g). $C_{26}H_{30}CdN_4O_6$ (606.94): calcd. C 51.45, H 4.98, N 9.23; found C 51.44, H 4.90, N 9.35. IR (KBr): $\tilde{\nu}$ = 3736 (w), 3597 (w), 2934 (w), 1676 (w), 1646 (m), 1623 (m), 1549 (s), 1512 (s), 1483 (s), 1415 (s), 1389 (s), 1304 (m), 1241 (w), 1126 (w), 744 (m), 674 (s), 425 (m) cm^{-1}.

Synthesis of [Cd(adi)(L^2)] (10): A mixture of $Cd(OH)_2$ (0.035 g, 0.2 mmol), H_2adi (0.029 g, 0.2 mmol), L^2 (0.069 g, 0.2 mmol) in EtOH/H_2O (1:4, v/v) (10 mL) was placed in a Teflon reactor. The mixture was heated at 180 °C for 3 d, and then it was gradually cooled to room temperature at a rate of 10 °C h^{-1}. Colorless crystals of **10** were obtained. Yield 53% based on $Cd(OH)_2$ (0.070 g). $C_{28}H_{34}CdN_4O_4$ (602.99): calcd. C 55.77, H 5.68, N 9.29; found C 55.68, H 5.60, N 9.33. IR (KBr): $\tilde{\nu}$ = 3847 (w), 3736 (s), 3621 (m), 1692 (m), 2926 (m), 1741 (m), 1646 (s), 1565 (m), 1548 (s), 1532 (m), 1512 (s), 1464 (w), 1061 (s), 673 (s), 604 (w), 483 (w) cm^{-1}.

Synthesis of [Cd(adi)(L^3)]·$2H_2O$ (11): A mixture of $Cd(OH)_2$ (0.035 g, 0.2 mmol), H_2adi (0.029 g, 0.2 mmol), L^3 (0.094 g, 0.2 mmol) in EtOH/H_2O (1:4, v/v) (10 mL) was placed in a Teflon reactor. The mixture was heated at 140 °C for 3 d, and then it was gradually cooled to room temperature at a rate of 10 °C h^{-1}. Colorless crystals of **11** were obtained. Yield 58% based on $Cd(OH)_2$ (0.070 g). $C_{38}H_{42}CdN_4O_6$ (763.16): calcd. C 59.80, H 5.55, N 7.34; found C 59.75, H 5.59, N 7.39. IR (KBr): $\tilde{\nu}$ = 3846 (w), 3736 (s), 3670 (m), 1742 (w), 1643 (s), 1547 (s), 1512 (s), 1462 (s), 1391 (s), 1242 (m), 1067 (m), 979 (m), 745 (m), 678 (s), 423 (w) cm^{-1}.

X-ray Crystallography: Single-crystal X-ray diffraction data for compounds **3** and **11** were recorded with a Bruker Apex CCD diffractometer with graphite-monochromated Mo-K_α radiation (λ = 0.71073 Å) at 293 K. Diffraction data for compounds **1**, **2**, and **4**–**10** were collected with a Rigaku RAXIS-RAPID single-crystal diffractometer with Mo-K_α radiation (λ = 0.71073 Å) at 293 K. Absorption corrections were applied using the multi-scan technique. All the structures were solved by direct methods using SHELXS-97[20] and refined by full-matrix least-squares techniques using the

Table 3. Crystal data and structure refinements for compounds **1**–**4**.

	1	**2**	**3**	**4**
Empirical formula	$C_{38}H_{38}N_4O_5Zn$	$C_{40}H_{40}N_4O_4Zn$	$C_{38}H_{38}CdN_4O_5$	$C_{40}H_{40}CdN_4O_4$
Formula mass	696.09	706.13	743.12	753.16
Crystal system	monoclinic	monoclinic	monoclinic	monoclinic
Space group	$P2/c$	$P2/c$	$P2/c$	$P2/c$
a [Å]	10.796(3)	10.861(4)	10.214(1)	11.290(5)
b [Å]	8.987(3)	8.856(3)	9.160(1)	9.000(3)
c [Å]	19.052(7)	19.466(6)	19.048(2)	18.711(6)
α [°]	90	90	90	90
β [°]	94.20(2)	95.51(2)	103.40(2)	94.67(2)
γ [°]	90	90	90	90
V [Å^3]	1843.5(11)	878.3(1)	1733.6(3)	1894.9(13)
Z	2	2	2	2
$D_{calcd.}$ [g cm^{-3}]	1.254	1.258	1.424	1.320
$F(000)$	728	740	764	776
Reflections collected/unique	17611/4196	17688/4241	10599/4194	18095/4323
GOF on F^2	1.037	1.042	1.046	1.077
R_1[a] [$I > 2\sigma(I)$]	0.0523	0.0651	0.0623	0.0479
wR_2[b]	0.1540	0.1659	0.1764	0.1352

[a] $R_1 = \Sigma||F_o| - |F_c||/\Sigma|F_o|$. [b] $wR_2 = |\Sigma w(|F_o|^2 - |F_c|^2)|/\Sigma|w(F_o^2)^2|^{1/2}$.

Table 4. Crystal data and structure refinements for compounds **5**–**8**.

	5	**6**	**7**	**8**
Empirical formula	$C_{16}H_{23}AgN_3O_4S$	$C_{17}H_{27}AgN_3O_5S$	$C_{26}H_{32}N_4O_5Zn$	$C_{17}H_{21}N_2O_4Zn$
Formula mass	461.30	493.35	545.93	382.73
Crystal system	monoclinic	monoclinic	triclinic	triclinic
Space group	$C2/c$	$P2_1/n$	$P\bar{1}$	$P\bar{1}$
a [Å]	21.379(9)	8.421(3)	8.459(5)	9.040(5)
b [Å]	9.867(3)	11.803(6)	9.507(7)	9.366(5)
c [Å]	19.558(6)	19.51(1)	17.48(1)	11.322(5)
α [°]	90	90	81.10(2)	81.10(2)
β [°]	117.36(1)	93.83(2)	84.06(2)	112.24(2)
γ [°]	90	90	69.11(2)	99.87(2)
V [Å^3]	3664(2)	1934.8(16)	1295.9(14)	835.9(7)
Z	8	4	2	2
$D_{calcd.}$ [g cm^{-3}]	1.672	1.694	1.399	1.521
$F(000)$	1880	1012	572	398
Reflections collected/unique	17527/4198	16479/4418	12669/5834	8208/3779
GOF on F^2	1.043	1.139	1.102	1.049
R_1[a] [$I > 2\sigma(I)$]	0.0252	0.0349	0.0920	0.0565
wR_2[b]	0.0610	0.0703	0.1827	0.0851

[a] $R_1 = \Sigma||F_o| - |F_c||/\Sigma|F_o|$. [b] $wR_2 = |\Sigma w(|F_o|^2 - |F_c|^2)|/\Sigma|w(F_o^2)^2|^{1/2}$.

Table 5. Crystal data and structure refinements for compounds **9**–**11**.

	9	**10**	**11**
Empirical formula	$C_{26}H_{34}CdN_4O_6$	$C_{28}H_{34}CdN_4O_4$	$C_{38}H_{42}CdN_4O_6$
Formula mass	610.97	602.99	763.16
Crystal system	triclinic	orthorhombic	monoclinic
Space group	$P\bar{1}$	*Pbca*	*Cc*
a [Å]	8.608(3)	18.294(3)	10.540(3)
b [Å]	9.584(4)	15.498(3)	22.909(4)
c [Å]	17.451(8)	19.285(4)	14.916(8)
a [°]	82.53(2)	90	90
β [°]	85.05(2)	90	102.09(2)
γ [°]	69.76(2)	90	90
V [Å^3]	1338.0(10)	5467.7(19)	3522(2)
Z	2	8	4
$D_{\text{calcd.}}$ [g cm^{-3}]	1.516	1.465	1.439
$F(000)$	628	2480	1576
Reflections collected/unique	13240/6061	48852/6232	10990/6306
GOF on F^2	1.064	1.023	0.987
R_1[a] [$I > 2\sigma(I)$]	0.0355	0.0355	0.0410
wR_2[b]	0.0888	0.0737	0.0760

[a] $R_1 = \Sigma||F_o| - |F_c||/\Sigma|F_o|$. [b] $wR_2 = |\Sigma w(|F_o|^2 - |F_c|^2)|/\Sigma|w(F_o^2)^2|^{1/2}$.

SHELXL-97 program.[21] Non-hydrogen atoms were refined with anisotropic temperature parameters. The disordered ligands in compounds **4**, **7**, and **9** were refined using isotropic C atoms split over two sites, with a total occupancy of 1. The hydrogen atoms of the organic ligands were refined as rigid groups. Some water H atoms in compound **11** could not be positioned reliably. Other H atoms of water molecules were located from difference Fourier maps. The detailed crystallographic data and structure refinement parameters for **1**–**11** are summarized in Tables 3, 4 and 5. Selected bond lengths and angles for compounds **1**–**11** are listed in Table S1 (see the Supporting Information).

CCDC-656673 (for **1**), -656674 (for **2**), -656675 (for **3**), -656676 (for **4**), -656677 (for **5**), -656678 (for **6**), -656679 (for **7**), -656680 (for **8**), -656681 (for **9**), -656682 (for **10**), -656683 (for **11**) contain the supplementary crystallographic data for this paper. These data can be obtained free of charge from The Cambridge Crystallographic Data Centre via www.ccdc.cam.ac.uk/data_request/cif.

Supporting Information (see also the footnote on the first page of this article): Selected bond lengths and angles. View of the infinite 1-D zigzag chain of compound **2**. Packing diagrams of compounds **3**, **4**, and **6**. TGA diagrams of compounds **1**, **3**, **7**, **9**, and **11**. The solid-state photoluminescent spectra of **1**–**11**, L^1, L^2, L^3, and the Hcin ligand.

Acknowledgments

We thank the National Natural Science Foundation of China (No. 20471014), Program for New Century Excellent Talents in Chinese University (NCET-05-0320), Program for Changjiang Scholars and Innovative Research Teams in Chinese University, the Science Foundation for Young Teachers of NENU (No. 20050310 and 20060304), and the Analysis and Testing Foundation of Northeast Normal University for support.

---

[1] a) S. Noro, S. Kitagawa, M. Kondo, K. Seki, *Angew. Chem. Int. Ed.* **2000**, *39*, 2081–2084; b) M. J. Zaworotko, *Chem. Soc. Rev.* **1994**, *23*, 283–288; c) O. M. Yaghi, H. Li, C. Davis, D. Richardson, T. L. Groy, *Acc. Chem. Res.* **1998**, *31*, 474–484; d) R. Robson, B. F. Abrahams, S. R. Batten, R. W. Gable, B. F. Hoskins, J. Liu, *Supramolecular Architecture*, American Chemical Society, Washington, DC, **1992**; e) J. M. Lehn, *Supramolecular Chemistry, Concepts and Perspectives*, VCH, Weinheim, Germany, **1995**, chapter 9; f) S. R. Batten, R. Robson, *Angew. Chem. Int. Ed.* **1998**, *37*, 1460–1494; g) P. J. Hagrman, D. Hagrman, J. Zubieta, *Angew. Chem. Int. Ed.* **1999**, *38*, 2638–2684; h) J. W. Steed, J. L. Atwood, *Supramolecular Chemistry*, Wiley, Chichester, U. K., **2000**; i) S. Subramanian, M. J. Zaworotko, *Coord. Chem. Rev.* **1994**, *137*, 357–401; j) B. J. Holliday, C. A. Mirkin, *Angew. Chem. Int. Ed.* **2001**, *40*, 2022–2043.

[2] a) R. Vilar, *Angew. Chem. Int. Ed.* **2003**, *42*, 1460–1477; b) B. Chen, F. R. Fronczek, A. W. Maverick, *Chem. Commun.* **2003**, 2166–2167; c) M. Yoshizawa, M. Nagao, K. Umemoto, K. Biradha, M. Fujita, S. Sakamoto, K. Yamaguchi, *Chem. Commun.* **2003**, 1808–1809; d) K. I. Nättinen, K. Rissanen, *Inorg. Chem.* **2003**, *42*, 5126–5134; e) D. Guo, K.-L. Pang, C.-Y. Duan, C. He, Q.-J. Meng, *Inorg. Chem.* **2002**, *41*, 5978–5985; f) C.-Y. Su, Y.-P. Cai, C.-L. Chen, F. Lissner, B.-S. Kang, W. Kaim, *Angew. Chem. Int. Ed.* **2002**, *41*, 3371–3375; g) S. Banfi, L. Carlucci, E. Caruso, G. Ciani, D. M. Proserpio, *J. Chem. Soc. Dalton Trans.* **2002**, 2714–2721; h) Z. Xu, S. Lee, Y.-H. Kiang, A. B. Mallik, N. Tsomaia, K. T. Mueller, *Adv. Mater.* **2001**, *13*, 637–641; i) O. R. Evans, W. Lin, *Chem. Mater.* **2001**, *13*, 2705–2712; j) N. P. Chatterton, D. M. L. Goodgame, D. A. Grachvogel, I. Hussain, A. J. P. White, D. J. Williams, *Inorg. Chem.* **2001**, *40*, 312–317; k) H. J. Choi, M. P. Suh, *J. Am. Chem. Soc.* **1998**, *120*, 10622–10628; l) C. M. Hartshorn, P. J. Steel, *J. Chem. Soc. Dalton Trans.* **1998**, 3927–3934.

[3] a) J. Lu, G. Crisci, T. Niu, A. J. Jacobson, *Inorg. Chem.* **1997**, *36*, 5140–5141; b) K. Biradha, G. Mahata, *Cryst. Growth Des.* **2005**, *5*, 61–63; c) R. P. Singh, J. M. Shreeve, *Inorg. Chem.* **2003**, *42*, 7416–7421; d) R. Dorta, R. Dorta, L. J. W. Shimon, D. Milstein, *Inorg. Chem.* **2004**, *43*, 7180–7186; e) A. J. Fletcher, E. J. Cussen, D. Bradshaw, M. J. Rosseinsky, K. M. Thomas, *J. Am. Chem. Soc.* **2004**, *126*, 9750–9759; f) K. Biradha, M. Sarkar, L. Rajput, *Chem. Commun.* **2006**, 4169–4179.

[4] a) T. Rajendran, B. Manimaran, R.-T. Liao, R.-J. Lin, P. Thanasekaran, G.-H. Lee, S.-M. Peng, Y.-H. Liu, I.-J. Chang, S. Rajagopal, K.-L. Lu, *Inorg. Chem.* **2003**, *42*, 6388–6394; b) S. A. Barnett, A. J. Blake, N. R. Champness, C. Wilson, *Dalton Trans.* **2005**, 3852–3861; c) E. Siebel, A. M. A. Ibrahim, R. D. Fischer, *Inorg. Chem.* **1999**, *38*, 2530–2532; d) D. Mandal, B. D. Gupta, *Eur. J. Inorg. Chem.* **2006**, 4086–4095; e) A. Neels, H. Stoeckli-Evans, *Inorg. Chem.* **1999**, *38*, 6164–6170.

[5] a) B. F. Hoskins, R. Robson, D. A. Slizys, *J. Am. Chem. Soc.* **1997**, *119*, 2952–2953; b) X.-H. Bu, W. Chen, W.-F. Hou, M. Du, R.-H. Zhang, F. Brisse, *Inorg. Chem.* **2002**, *41*, 3477–3482;

c) L. Carlucci, G. Ciani, D. M. Proserpio, S. Rizzato, *CrystEngComm* **2002**, *4*, 413–425; d) X. Meng, Y. Song, H. Hou, Y. Fan, G. Li, Y. Zhu, *Inorg. Chem.* **2003**, *42*, 1306–1315; e) R. Gupta, R. Mukherjee, *Polyhedron* **2000**, *19*, 719–724; f) L. Carlucci, G. Ciani, D. M. Proserpio, *Cryst. Growth Des.* **2005**, *5*, 37–39.

[6] a) J.-F. Ma, J.-F. Liu, Y. Xing, H.-Q. Jia, Y.-H. Lin, *J. Chem. Soc. Dalton Trans.* **2000**, 2403–2407; b) J.-F. Ma, J.-F. Liu, Y.-C. Liu, Y. Xing, H.-Q. Jia, Y.-H. Lin, *New J. Chem.* **2000**, *24*, 759–763; c) J.-F. Ma, J. Yang, S.-L. Li, S.-Y. Song, H.-J. Zhang, H.-S. Wang, K.-Y. Yang, *Cryst. Growth Des.* **2005**, *5*, 807–812; d) F.-F. Li, J.-F. Ma, S.-Y. Song, J. Yang, Y.-Y. Liu, Z.-M. Su, *Inorg. Chem.* **2005**, *44*, 9374–9383; e) F.-F. Li, J.-F. Ma, S.-Y. Song, J. Yang, H.-Q. Jia, N.-H. Hu, *Cryst. Growth Des.* **2006**, *6*, 209–215.

[7] a) P. C. Srivastava, S. Bajpai, S. Bajpai, R. Kumar, R. J. Butcher, *Inorg. Chim. Acta* **2005**, *358*, 227–232; b) A. K. Ghosh, D. Ghoshal, J. Ribas, G. Mostafa, N. R. Chaudhuri, *Cryst. Growth Des.* **2006**, *6*, 36–39; c) L. A. Borkowski, C. L. Cahill, *Inorg. Chem.* **2003**, *42*, 7041–7045; d) Y.-Q. Zheng, J.-L. Lin, Z.-P. Kong, *Inorg. Chem.* **2004**, *43*, 2590–2596.

[8] a) S. Das, P. K. Bharadwaj, *Cryst. Growth Des.* **2006**, *6*, 187–192; b) S. G. Ang, B. W. Sun, *Cryst. Growth Des.* **2005**, *5*, 383–386; c) O. R. Evans, W. Lin, *Cryst. Growth Des.* **2001**, *1*, 9–11.

[9] G. S. Papaefstathiou, Z. Zhong, L. Geng, L. R. MacGillivray, *J. Am. Chem. Soc.* **2004**, *126*, 9158–9159.

[10] a) G. A. Jeffrey, H. Maluszynska, *Acta Crystallogr., Sect. B* **1990**, *46*, 546–549; b) M. Wei, C. He, W. Hua, C. Duan, S. Li, Q. Meng, *J. Am. Chem. Soc.* **2006**, *128*, 13318–13319; c) S. K. Ghosh, P. K. Bharadwaj, *Eur. J. Inorg. Chem.* **2005**, 4880–4885; d) J. M. Ugalde, I. Alkorta, J. Elguero, *Angew. Chem. Int. Ed.* **2000**, *39*, 717–721; e) R. Ludwig, *Angew. Chem. Int. Ed.* **2001**, *40*, 1808–1827; f) S. Wang, H. Xing, Y. Li, J. Bai, Y. Pan, M. Scheer, X. You, *Eur. J. Inorg. Chem.* **2006**, *15*, 3041–3053.

[11] a) X.-L. Wang, C. Qin, E.-B. Wang, *Cryst. Growth Des.* **2006**, *6*, 439–443; b) X.-L. Wang, C. Qin, E.-B. Wang, L. Xu, *Cryst. Growth Des.* **2006**, *6*, 2061–2065; c) X.-L. Wang, C. Qin, E.-B. Wang, Z.-M. Su, *Chem. Eur. J.* **2006**, *12*, 2680–2691; d) M. A. Withersby, A. J. Blake, N. R. Champness, P. Hubberstey, W.-S. Li, M. Schröder, *Angew. Chem. Int. Ed. Engl.* **1997**, *36*, 2327–2329; e) L. Carlucci, G. Ciani, P. Macchi, D. M. Proserpio, S. Rizzato, *Chem. Eur. J.* **1999**, *5*, 237–243; f) E. Y. Lee, M. P. Suh, *Angew. Chem. Int. Ed.* **2004**, *43*, 2798–2801.

[12] a) E. T. Kefalas, M. Dakanali, P. Panagiotidis, C. P. Raptopoulou, A. Terzis, T. Mavromoustakos, I. Kyrikou, N. Karligiano, A. Bino, A. Salifoglou, *Inorg. Chem.* **2005**, *44*, 4818–4828; b) W. Clegg, J. T. Cressey, A. McCamley, B. P. Straughan, *Acta Crystallogr., Sect. C* **1995**, *51*, 234–235.

[13] G. K. H. Shimizu, G. D. Enright, C. I. Ratcliffe, G. S. Rego, J. L. Reid, J. A. Ripmeester, *Chem. Mater.* **1998**, *10*, 3282–3283.

[14] a) V. A. Blatov, L. Carlucci, G. Ciani, D. M. Proserpio, *CrystEngComm* **2004**, *6*, 378–395; b) K. Liang, H. Zheng, Y. Song, M. F. Lappert, Y. Li, X. Xin, Z. Huang, J. Chen, S. Lu, *Angew. Chem. Int. Ed.* **2004**, *43*, 5776–5779; c) K. M. E. Jones, A. H. Mahmoudkhani, B. D. Chandler, G. K. H. Shimizu, *CrystEngComm* **2006**, *8*, 303–305; d) R.-Q. Zou, Y. Yamada, Q. Xu, *Microporous Mesoporous Mater.* **2006**, *91*, 233–237; e) M. A. Withersby, A. J. Blake, N. R. Champness, P. A. Cooke, P. Hubberstey, A. L. Realf, S. J. Teat, M. Schröder, *J. Chem. Soc. Dalton Trans.* **2000**, 3261–3268; f) X.-J. Li, R. Cao, W.-H. Bi, Y.-Q. Wang, Y.-L. Wang, X. Li, *Polyhedron* **2005**, *24*, 2955–2962; g) Y.-H. Liu, H.-C. Wu, H.-M. Lin, W.-H. Hou, K.-L. Lu, *Chem. Commun.* **2003**, 60–61; h) J.-P. Zhang, S. Horike, S. Kitagawa, *Angew. Chem. Int. Ed.* **2007**, *46*, 889–892.

[15] a) E. G. Bakalbassis, M. Korabik, A. Michailides, J. Mrozinski, C. Raptopoulou, S. Skoulika, A. Terzis, D. Tsaousis, *J. Chem. Soc. Dalton Trans.* **2001**, 850–861; b) J. Fan, W.-Y. Sun, T.-A. Okamura, Y.-Q. Zheng, B. Sui, W.-X. Tang, N. Ueyama, *Cryst. Growth Des.* **2004**, *4*, 579–584.

[16] Z. Huang, H.-B. Song, M. Du, S.-T. Chen, X.-H. Bu, J. Ribas, *Inorg. Chem.* **2004**, *43*, 931–944.

[17] a) J. E. McGarrah, Y.-J. Kim, M. Hissler, R. Eisenberg, *Inorg. Chem.* **2001**, *40*, 4510–4511; b) G. D. Santis, L. Fabbrizzi, M. Licchelli, A. Poggi, A. Taglietti, *Angew. Chem. Int. Ed. Engl.* **1996**, *35*, 202–204; c) Q. Wu, M. Esteghamatian, N.-X. Hu, Z. Popovic, G. Enright, Y. Tao, M. D′Iorio, S. Wang, *Chem. Mater.* **2000**, *12*, 79–83.

[18] a) V. W.-W. Yam, K. K.-W. Lo, *Chem. Soc. Rev.* **1999**, *28*, 323–334; b) N. Kaltsoyannis, *J. Chem. Soc. Dalton Trans.* **1997**, 1–12; c) S.-L. Zheng, J.-H. Yang, X.-L. Yu, X.-M. Chen, W.-T. Wong, *Inorg. Chem.* **2004**, *43*, 830–838; d) H. Kunkely, A. Vogler, *J. Chem. Soc. Chem. Commun.* **1990**, 1204–1205.

[19] a) Y. Kang, C. Seward, D. Song, S. Wang, *Inorg. Chem.* **2003**, *42*, 2789–2797; b) X.-M. Zhang, M.-L. Tong, M.-L. Gong, X.-M. Chen, *Eur. J. Inorg. Chem.* **2003**, 138–142.

[20] G. M. Sheldrick, *SHELXS-97*, Program for X-ray Crystal Structure Solution, University of Göttingen, Göttingen, **1997**.

[21] G. M. Sheldrick, *SHELXL-97*, Programs for X-ray Crystal Structure Refinement, University of Göttingen, Göttingen, Germany, **1997**.

Received: August 8, 2007